World Journal of Diabetes

Submit a Manuscript: https://www.f6publishing.com

World J Diabetes 2024 April 15; 15(4): 769-782

DOI: 10.4239/wjd.v15.i4.769

ISSN 1948-9358 (online)

ORIGINAL ARTICLE

Basic Study

Icariin accelerates bone regeneration by inducing osteogenesis-angiogenesis coupling in rats with type 1 diabetes mellitus

Sheng Zheng, Guan-Yu Hu, Jun-Hua Li, Jia Zheng, Yi-Kai Li

Specialty type: Endocrinology and metabolism

Provenance and peer review: Invited article; Externally peer reviewed.

Peer-review model: Single blind

Peer-review report's scientific quality classification

Grade A (Excellent): 0
Grade B (Very good): B
Grade C (Good): C
Grade D (Fair): 0
Grade E (Poor): 0

P-Reviewer: Sanyal D, India; Papazafiropoulou A, Greece

Received: December 31, 2023
Peer-review started: December 31, 2023
First decision: January 16, 2024
Revised: January 22, 2024
Accepted: March 5, 2024
Article in press: March 5, 2024
Published online: April 15, 2024

Sheng Zheng, Guan-Yu Hu, Yi-Kai Li, Department of Traditional Chinese Orthopedics and Traumatology, Center for Orthopedic Surgery, The Third Affiliated Hospital of Southern Medical University, Guangzhou 510630, Guangdong Province, China

Jun-Hua Li, School of Traditional Chinese Medicine, Southern Medical University, Guangzhou 510515, Guangdong Province, China

Jia Zheng, Department of Endocrinology, Peking University First Hospital, Beijing 100034, China

Corresponding author: Yi-Kai Li, MD, PhD, Chief Physician, Full Professor, Professor, Research Scientist, Department of Traditional Chinese Orthopedics and Traumatology, Center for Orthopedic Surgery, The Third Affiliated Hospital of Southern Medical University, No. 183 Zhongshan Avenue West, Tianhe District, Guangzhou 510630, Guangdong Province, China. ortho@smu.edu.cn

Abstract

BACKGROUND

Icariin (ICA), a natural flavonoid compound monomer, has multiple pharmacological activities. However, its effect on bone defect in the context of type 1 diabetes mellitus (T1DM) has not yet been examined.

AIM

To explore the role and potential mechanism of ICA on bone defect in the context of T1DM.

METHODS

The effects of ICA on osteogenesis and angiogenesis were evaluated by alkaline phosphatase staining, alizarin red S staining, quantitative real-time polymerase chain reaction, Western blot, and immunofluorescence. Angiogenesis-related assays were conducted to investigate the relationship between osteogenesis and angiogenesis. A bone defect model was established in T1DM rats. The model rats were then treated with ICA or placebo and micron-scale computed tomography, histomorphometry, histology, and sequential fluorescent labeling were used to evaluate the effect of ICA on bone formation in the defect area.

RESULTS

ICA promoted bone marrow mesenchymal stem cell (BMSC) proliferation and

osteogenic differentiation. The ICA treated-BMSCs showed higher expression levels of osteogenesis-related markers (alkaline phosphatase and osteocalcin) and angiogenesis-related markers (vascular endothelial growth factor A and platelet endothelial cell adhesion molecule 1) compared to the untreated group. ICA was also found to induce osteogenesis-angiogenesis coupling of BMSCs. In the bone defect model T1DM rats, ICA facilitated bone formation and CD31^{hi}EMCN^{hi} type H-positive capillary formation. Lastly, ICA effectively accelerated the rate of bone formation in the defect area.

CONCLUSION

ICA was able to accelerate bone regeneration in a T1DM rat model by inducing osteogenesis-angiogenesis coupling of BMSCs.

Key Words: Icariin; Osteogenesis-angiogenesis coupling; Type 1 diabetes mellitus; Bone defect; Bone regeneration

Core Tip: Type 1 diabetes mellitus (T1DM) leads to a decrease in bone formation in a bone defect area. We demonstrated that icariin, a natural flavonoid compound monomer, accelerated bone regeneration by inducing osteogenesis-angiogenesis coupling of bone marrow mesenchymal stem cells in a T1DM rat model. This finding indicates that further investigations into the effective coupling of osteogenesis and angiogenesis should be undertaken in the field of bone regeneration in T1DM patients.

Citation: Zheng S, Hu GY, Li JH, Zheng J, Li YK. Icariin accelerates bone regeneration by inducing osteogenesis-angiogenesis coupling in rats with type 1 diabetes mellitus. *World J Diabetes* 2024; 15(4): 769-782
URL: https://www.wjgnet.com/1948-9358/full/v15/i4/769.htm
DOI: https://dx.doi.org/10.4239/wjd.v15.i4.769

INTRODUCTION

Diabetes mellitus (DM) is a growing epidemic globally[1]. Worldwide, about 463 million adults aged 20 years to 79 years are suffering from diabetes, with a prevalence rate of 9.3%. It is estimated that by 2030 there will be 578 million (10.2%) people living with DM[2]. DM places a significant strain on medical resources and patient quality of life, which in turn places heavy burdens on society and the patient's family[3]. DM is typically categorized as type 1 DM (T1DM) and type 2 DM based on the etiology. Patients with T1DM require exogenous insulin to lower blood glucose. Otherwise, chronic high blood glucose can lead to damage in the heart, blood vessels, eyes, kidneys and nerves[4]. A growing body of research has shown T1DM affects bone metabolism[5-7]; however, the underlying mechanism has not yet been fully elucidated.

Although the bone has a propensity for repairing itself, cases arise that are beyond the self-repairing capacity of the bone[8]. One of these cases is a bone defect in a patient with T1DM[9]. Bone metabolism is disordered in T1DM, which increases the challenges for the treatment of bone defects[10-12]. The current standard of treatment are allografts and autografts. However, patients find these therapies to be unsatisfactory[13]. Studies have suggested that the pathogenesis of disordered bone metabolism caused by T1DM is closely related to the imbalance between bone resorption and bone formation, and a high glucose environment could significantly inhibit osteoblast-mediated bone formation and promote osteoclast-mediated bone absorption[14-16].

Icariin (ICA) is a natural flavonol glycoside primarily extracted from *Herba Epimedii*. It has multiple pharmacological activities, including anti-inflammatory, anti-rheumatic, anti-diabetic nephropathy, anti-apoptotic, and anti-oxidative properties[17-21]. ICA can also promote osteogenesis and play an anti-osteoporotic role[22-24]. Huang *et al*[25] showed that ICA promoted osteogenic differentiation through upregulation of BMAL1, and Cheng *et al*[26] demonstrated that ICA attenuated thioacetamide-induced bone loss through downregulation of the RANKL-p38/ERK-NFAT pathway. Hao *et al*[27] observed that ICA accelerated bone regeneration in the defect area of rabbit skulls. Several other studies have demonstrated the protective effects of ICA in T1DM models[28-30]. Considering these findings collectively, we hypothesize that ICA has therapeutic potential for bone defect repair in T1DM.

Both osteogenesis and angiogenesis exert vital roles during the bone regeneration process[28-31]. Several studies have consistently demonstrated the ability of ICA to promote osteogenesis[32-34]. Interestingly, ICA has been shown to play different roles in angiogenesis depending on the circumstances. Yu *et al*[35] reported that ICA promoted angiogenesis in glucocorticoid-induced osteonecrosis of femoral heads, and Huang *et al*[36] demonstated ICA inhibition of angiogenesis *via* regulation of the TDP-43 signaling pathway. It is unknown how ICA affects angiogenesis during the bone regeneration process in the context of T1DM. Therefore, this study investigated the effects and potential mechanisms of ICA on bone defect repair in the context of T1DM.

MATERIALS AND METHODS

Chemicals and reagents

ICA (Cat. No. M211098) was ordered from Mreda Technology Co., Ltd. (Beijing, China). Monoclonal antibodies against CD29 (Cat. No. 11-0291-82), CD90 (Cat. No. 11-0900-81), CD105 (Cat. No. MA1-19594), CD34 (Cat. No. 11-0341-85), and CD45 (Cat. No. 11-0461-82) were purchased from eBioscience (San Diego, CA, United States). Primary antibodies against alkaline phosphatase (ALP; Cat. No. DF6225), osteocalcin (OCN; Cat. No. DF12303), vascular endothelial growth factor A (VEGFA; Cat. No. AF5131), and platelet endothelial cell adhesion molecule 1 (CD31; Cat. No. AF6191) were obtained from Affinity Biosciences (Cincinnati, OH, United States). The primary antibody against endomucin (EMCN; Cat. No. sc-65495) was obtained from Santa Cruz Biotechnology (Dallas, TX, United States).

Cell proliferation assay

Rat bone marrow mesenchymal stem cells (BMSCs) were isolated and cultured as previously described[37]. For phenotypic analysis, expression of CD29, CD90, CD105, CD34, and CD45 was evaluated. Cell counting kit-8 (CCK-8; Cat. No. C0039, Beyotime, Beijing, China) was used to evaluate the effect of ICA on BMSC proliferation. BMSCs were treated with different concentrations of ICA (0 μM, 1 μM, 10 μM, and 100 μM) for 1 d, 3 d, 5 d, and 7 d. The untreated group served as control (CON).

Colony-forming unit assay

BMSCs were seeded into 6-well plates (1×10^3 cells/well) and incubated in the presence or absence of ICA for 1 wk. Then, the clones were fixed with 4% paraformaldehyde and stained with 0.1% crystal violet for 20 min. Colonies containing 50 or more cells were quantified by ImageJ software (Release 1.51, National Institutes of Health, Bethesda, MD, United States).

Osteogenic differentiation assays

When BMSC confluency reached 80%, the medium was replaced with osteogenic medium. Varying concentrations of ICA were added. Total cellular proteins were extracted, and the supernatant liquid was collected for downstream assays. ALP activity was measured with an ALP Staining Kit (Beyotime) after 1 wk. Calcium mineralization was detected after 3 wk *via* alizarin red S (ARS) solution (Beyotime).

Quantitative real-time polymerase chain reaction

Total RNA was extracted with an RNA Purification Kit (Thermo Fisher Scientific, Waltham, MA, United States), and reverse transcription was performed with a cDNA Reverse Transcription Kit (Thermo Fisher Scientific). Quantitative real-time polymerase chain reaction (qRT-PCR) was performed using SYBR Green qPCR Master Mix (Thermo Fisher Scientific). Relative gene expression was calculated using the $2^{-\Delta\Delta CT}$ method. The primer sequences are listed in Table 1.

Western blot

Total protein was extracted using RIPA lysis buffer with protease inhibitors and protein phosphatase inhibitors (Beyotime) on ice. The cell lysates were collected and ultrasonicated for 10 min. After 15 min of centrifugation (4 °C, 12000 rpm), the protein concentration was measured with a BCA Protein Assay Kit (Beyotime). Equal amounts of protein (30 μg) were subjected to 10% SDS-PAGE and transferred to PVDF membranes (Serva Electrophoresis GmbH, Heidelberg, Germany). The membranes were incubated with primary antibodies against ALP (1:1000 dilution), OCN (1:1000), VEGFA (1:1000), CD31 (1:2000), and β-actin (1:5000). The proteins were visualized by autoradiography and analyzed with ImageJ software.

Immunofluorescence

BMSCs were fixed with 4% paraformaldehyde for 30 min, permeabilized with 0.5% Triton X-100 for 15 min, and blocked with 1% bovine serum albumin for 30 min. The cells were incubated with primary antibodies overnight at 4 °C. Subsequently, BMSCs were washed thrice with PBS and incubated with fluorescence-conjugated secondary antibodies for 2 h. Fluorescence images were obtained with a BX63 fluorescence microscope (Olympus, Tokyo, Japan).

Angiogenesis-related assays

To further evaluate the proangiogenesis ability of ICA, BMSCs were treated with 10 μM ICA for 1 wk, and the conditioned medium (CM) was harvested. Human umbilical vein endothelial cells (HUVECs) were also cultured under different conditions: (1) Fresh medium (FM) without ICA (FM + CON group); (2) FM with 1 μM ICA (FM + ICA group); (3) CM without ICA (CM + CON group); and (4) CM with 1 μM ICA (CM + ICA group). HUVECs (Cat. No. iCell-h110) were obtained from iCell Bioscience Inc (Shanghai, China).

The scratch wound assay was conducted with HUVECs seeded into 12-well plates at 2×10^5 cells/well. After confluence, the cells were scratched with a sterile yellow pipette tip and then cultured in the conditions listed above. Images of the wound were taken immediately and 24 h later. Images were analyzed by ImageJ software.

The transwell migration assay was conducted with HUVECs seeded into the upper chamber of 24-well transwell plates (BD Biosciences, Franklin Lakes, NJ, United States) at 3×10^5 cells/well. The culture conditions listed above were added to the lower chamber. After 12 h, the cells that migrated to the lower chamber surface were stained with 0.1% crystal violet for 30 min and measured upon visualization with an inverted microscope (IX73, Olympus).

The tube formation assay was conducted with HUVECs seeded into matrigel precoated 96-well plates at 1.5 × 10^4 cells/well. After 8 h of culture, tube formation was observed *via* an inverted microscope.

Surgery and treatment

Male Wistar rats (280 g ± 15 g; 8-wk-old; Laboratory Animal Center of Southern Medical University, Guangzhou, China) were used in this study. All animal experiments were reviewed and approved by the Animal Ethics Committee of Southern Medical University (Approval No. SMUL2022023, Date of approval: 16 November 2022, Guangzhou, China). All rats were housed in 55% humidity and 22 °C constant temperature under 12-h dark/light cycles. After 1 wk of adaptation, rats in the model group received intraperitoneal injections of streptozotocin (65 mg/kg) as previously described[38] to induce T1DM. Rats in the CON group received vehicle injections.

Blood glucose concentrations were evaluated after 3 d and 7 d. If the blood glucose concentration was higher than 16.7 mmol/L, the rats were diagnosed with T1DM and selected for further studies. Then, the T1DM rats and CON rats were weighed and anesthetized with pentobarbital sodium. The longitudinal approach was used to expose the right proximal tibial metaphysis. A standardized drill hole defect (4 mm diameter and 5 mm deep) was used to create a monocortical defect.

After surgery, according to the random number table method, the T1DM rats were classified into the following two groups: T1DM group (n = 32) and ICA group (n = 32). Rats in the control group were regarded as the CON group (n = 32). The ICA group was treated with ICA (100 mg/kg/d) by gavage for 4 wk, and the rats in the CON group and the T1DM group were treated with equal amounts of normal saline for 4 wk. The therapeutic dose of ICA was determined based on previous experiments where ICA showed protective effects in T1DM rats[39].

Micron-scale computed tomography

Bone repair was evaluated by micron-scale computed tomography (micro-CT; Bruker, Kontich, Belgium). The region of interest was first defined as the bone defect area. After three-dimensional reconstruction, the parameters of bone mineral density, bone volume/tissue volume, trabecular number, and trabecular separation were measured by micro-CT.

Histology staining

After micro-CT imaging, the tibias were decalcified in 10% EDTA for 21 d for subsequent histological analysis. Hematoxylin and eosin staining and Masson's trichrome staining were performed on 5 μm-thick sections. For immunohistochemical staining, 6 μm-thick sections were incubated with primary antibodies against OCN (1:100), VEGFA (1:200), and CD31 (1:200). For immunofluorescence staining, 4 μm-thick sections were incubated with primary antibodies against CD31 (1:500) and EMCN (1:100). Staining was visualized using the BX63 fluorescence microscope.

Sequential fluorescent labeling

All rats were injected subcutaneously with 10 mg/kg calcein (Sigma-Aldrich, St Louis, MO, United States) at 10 d and 3 d before sacrifice[40]. Fluorescent agents were freshly prepared before injection and filtered through a 0.45-μm filter. Tibia samples from each group were collected for hard-tissue slicing and imaged by laser confocal microscopy (FV3000, Olympus).

Statistical analysis

Statistical significance was assessed using two-tailed Student's t-test or analysis of variance. All statistical analyses were performed using SPSS software version 26.0 (IBM Corp., Armonk, NY, United States). Differences were considered statistically significant when the P value was < 0.05. Data were summarized as mean ± SEM.

RESULTS

ICA promoted BMSC proliferation and osteogenic differentiation

Flow cytometry of BMSCs confirmed their identity *via* positive expression for CD29 (99.70%), CD90 (99.51%), and CD105 (99.29%) and negative expression for CD34 (0.94%) and CD45 (0.78%) (Figure 1A). The CCK-8 assay indicated that ICA (Figure 1B) promoted BMSC proliferation at certain concentrations; however, the high concentration (100 μM) showed an inhibitory effect on BMSC proliferation (Figure 1C). The proliferation-promoting concentrations (1 μM and 10 μM) were confirmed by colony forming unit assay (Figure 1D and E). Next, we evaluated the osteogenic ability of ICA *via* ALP and ARS staining. The groups treated with ICA had higher ALP activity, and the optimal concentration was 10 μM (Figure 1F and G). The ICA-treated BMSCs showed more calcium nodule deposits, and the optimal concentration was 10 μM (Figure 1H and I).

ICA enhanced expression of osteogenesis-related and angiogenesis-related markers

After 3 d of incubation in ICA, the gene expression levels of osteogenesis-related markers were evaluated by qRT-PCR. The expression levels of *ALP* and *OCN* were elevated in the ICA-treated groups, but the expression levels of runt-related transcription factor 2 and collagen type I alpha 1 were not significantly different from those in the CON group (Figure 2A). After 1 wk of incubation, the protein levels of ALP and OCN were also elevated in the ICA-treated groups (Figure 2B). Furthermore, immunofluorescence staining of ALP and OCN confirmed these findings (Figure 2C and D). The optimal concentration of ICA was 10 μM, which was consistent with qRT-PCR and western blot. These results

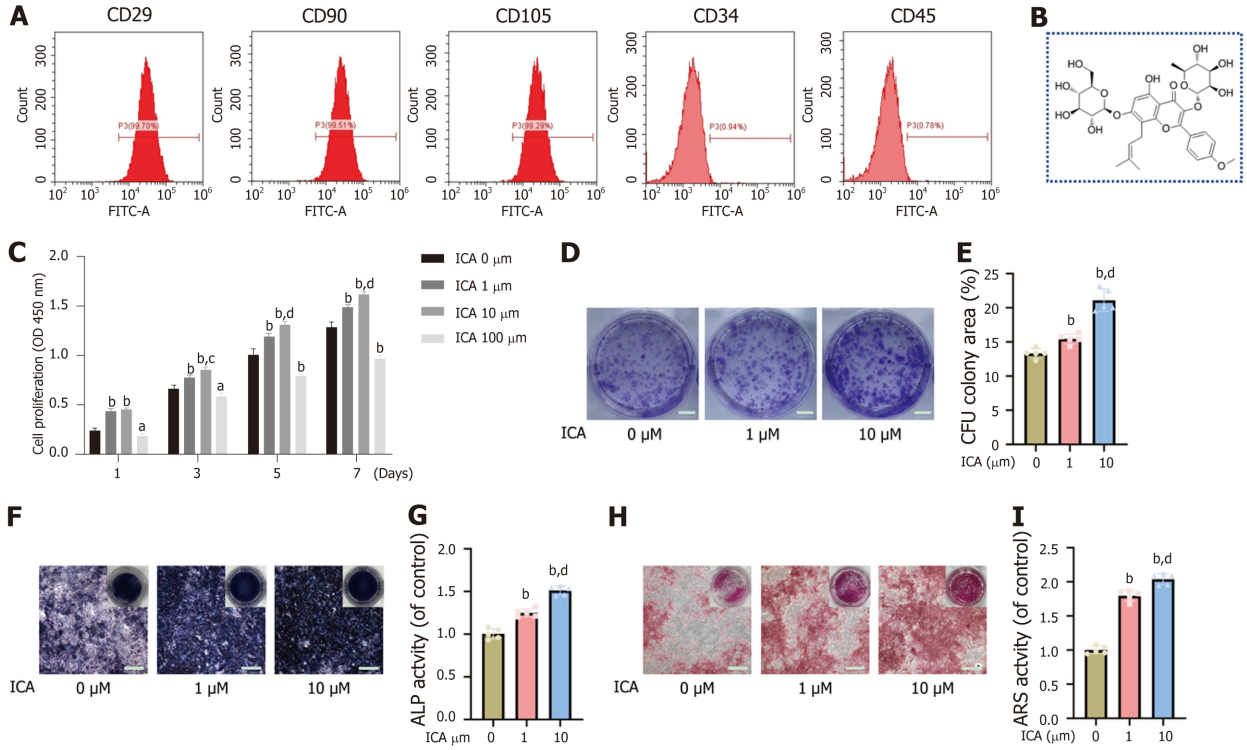

Figure 1 Icariin promoted bone marrow mesenchymal stem cell proliferation and osteogenic differentiation. A: Bone marrow mesenchymal stem cell (BMSC) surface markers were detected by flow cytometry; B: Icariin (ICA) chemical structure; C: The effect of ICA on BMSC proliferation was measured by the cell counting kit-8 assay; D: Representative images of the colony-forming unit (CFU) assay to determine the effect of ICA on BMSC proliferation; E: Quantification of the CFU assay; F: Representative images of alkaline phosphatase (ALP) staining (scale bar: 250 μm); G: ALP activity detection; H: Representative images of alizarin red S (ARS) staining (scale bar: 250 μm); I: Semi-quantitative result of ARS staining. Data are mean ± SEM (n = 5). $^{a}P < 0.05$ and $^{b}P < 0.01$ *vs* control group; $^{c}P < 0.05$ and $^{d}P < 0.01$ *vs* 1 μM ICA group. ICA: Icariin.

suggested that ICA enhanced the expression of osteogenesis-related markers.

After 3 d of incubation in ICA, the gene expression levels of angiogenesis-related markers were evaluated by qRT-PCR. The expression levels of *VEGFA* and *CD31* were elevated in the ICA-treated groups. However, the expression levels of angiopoietin-2 and angiopoietin-4 detected in the ICA-treated groups were not significantly different from those in the CON group (Figure 3A). After 1 wk of incubation, the protein expression levels of VEGFA and CD31 were also elevated in the ICA-treated groups (Figure 3B). Immunofluorescence staining of VEGFA and CD31 confirmed that ICA enhanced the expression of VEGFA and CD31 (Figure 3C and D). Significantly, the optimal concentration of ICA was also 10 μM. This indicates that the optimal concentration of ICA for promoting osteogenesis and angiogenesis was the same.

ICA induced osteogenesis-angiogenesis coupling of BMSCs

To further evaluate the proangiogenic ability of ICA, HUVECs were assessed *via* angiogenesis-related assays. The results of the scratch wound assay revealed that there was no significant difference in HUVEC migration between the FM + CON group and the FM + ICA group ($P > 0.05$). Interestingly, HUVEC migration was enhanced in the CM + CON group compared to the FM + CON group, as well as in the CM + ICA group compared to the CM + CON group (Figure 4A and B). This migration capacity was confirmed by transwell migration assay (Figure 4C and D). In addition, there were no differences in tube formation in HUVECs of the FM + CON group and FM + ICA group ($P > 0.05$). However, CM increased tube formation, and this effect was even greater in the CM + ICA group compared to the CM + CON group (Figure 4E and F). These findings imply that ICA does not promote angiogenesis in HUVECs in a direct manner but that it can promote angiogenesis in a BMSC-mediated manner. Therefore, the pro-osteogenic effect of ICA is coupled with its proangiogenesis effect.

ICA improved bone repair capacity by promoting osteogenesis in T1DM rats

After the tibial defect operation, the rats received ICA for 4 wk. The effect of ICA on bone defect repair was evaluated after 2 wk and 4 wk of the ICA treatment. The three-dimensional reconstruction revealed that ICA enlarged the area of bone regeneration at both time points (Figure 5A and B). Hematoxylin and eosin staining and Masson's trichrome staining confirmed these results (Figure 5C-F). Accordingly, further quantitative analysis of the defect area revealed that the values of bone mineral density, bone volume/tissue volume, and trabecular number were lowest in the T1DM group, and the value of trabecular separation was highest in the T1DM group (Figure 5G). Thus, while T1DM led to a decrease in bone formation in the tibial defects in this rat model, ICA could improve the bone repair capacity by promoting osteogenesis in the bone defect area.

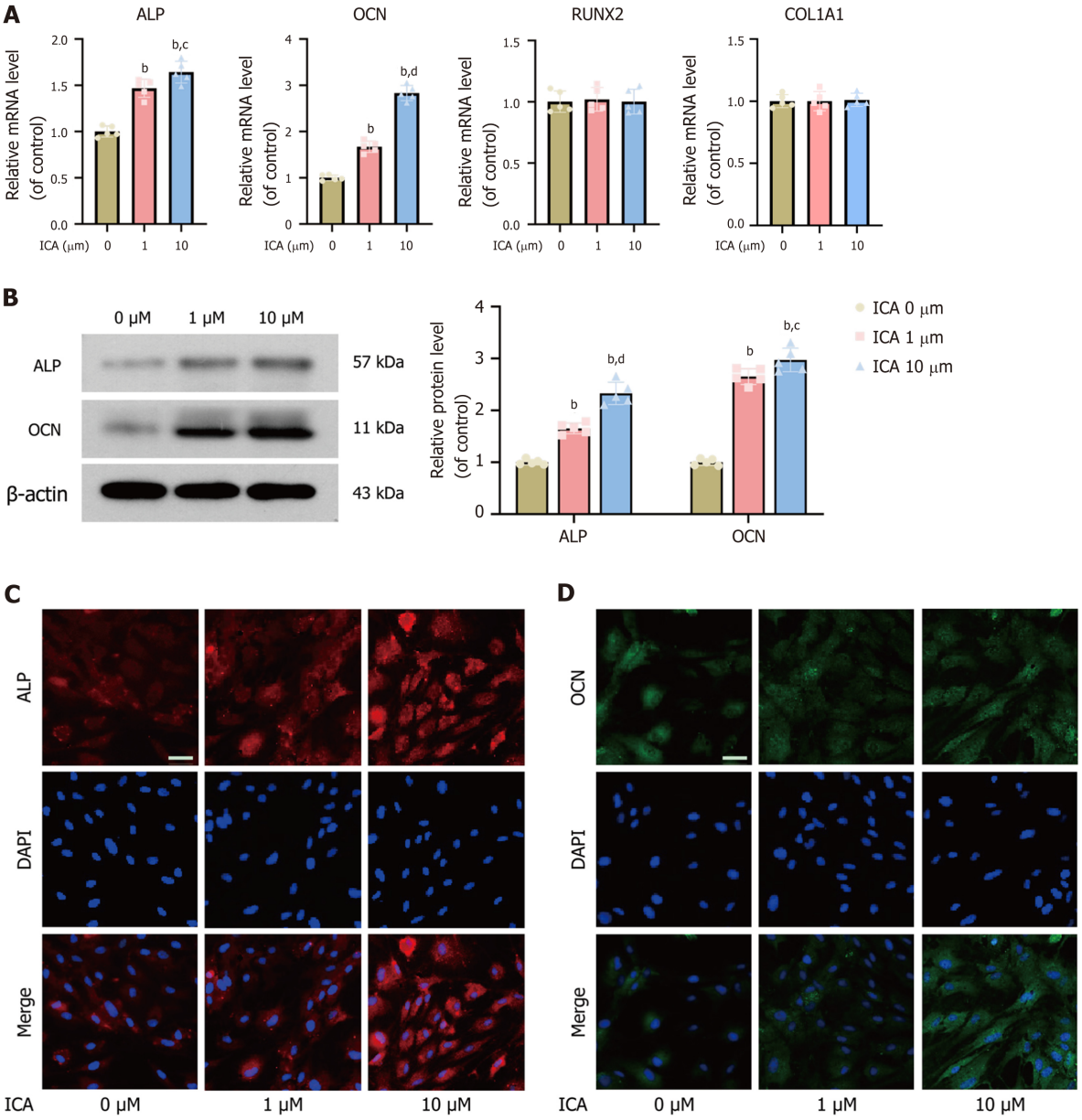

Figure 2 Icariin enhanced the expression of osteogenesis-related markers. A: Expression levels of osteogenesis-related genes [alkaline phosphatase (*ALP*), osteocalcin (*OCN*), runt-related transcription factor 2 (*RUNX2*), and collagen type I alpha 1 (*COL1A1*)] in bone marrow mesenchymal stem cells (BMSCs) following treatment with icariin (ICA); B: Protein expression levels of ALP and OCN by Western blot; C: Expression of ALP by immunofluorescence (scale bar: 100 μm); D: Expression of OCN by immunofluorescence (scale bar: 100 μm). Data are mean ± SEM (n = 5). $^{b}P < 0.01$ *vs* control group; $^{c}P < 0.05$ and $^{d}P < 0.01$ *vs* 1 μM ICA group. ICA: Icariin; ALP: Alkaline phosphatase; OCN: Osteocalcin; RUNX2: Runt-related transcription factor 2; COL1A1: Collagen type I alpha 1; qRT-PCR: Quantitative real-time polymerase chain reaction.

ICA accelerated bone regeneration by inducing osteogenesis-angiogenesis coupling of BMSCs in T1DM rats

At week 2, immunohistochemical staining of the osteogenesis-related marker OCN and the angiogenesis-related markers VEGFA and CD31 revealed an increase in these markers in the ICA group compared to those in the T1DM group (Figure 6A-C). At week 4, the same trend was observed for these markers (Figure 6D-F). The CD31 and EMCN double immunofluorescence staining revealed that ICA facilitated CD31^{hi}EMCN^{hi} type H-positive capillary formation in the bone defect area at both time points (Figure 6G and H). Furthermore, sequential fluorescent labeling revealed that the distance between double labels was wider in the ICA group than in the T1DM group (Figure 6I), which indicated that ICA accelerated the rate of bone formation in the defect area. Quantitative analysis of the bone mineral apposition rate confirmed the above finding (Figure 6J), indicating that ICA accelerated bone regeneration by inducing the osteogenesis-angiogenesis coupling in the T1DM rat model.

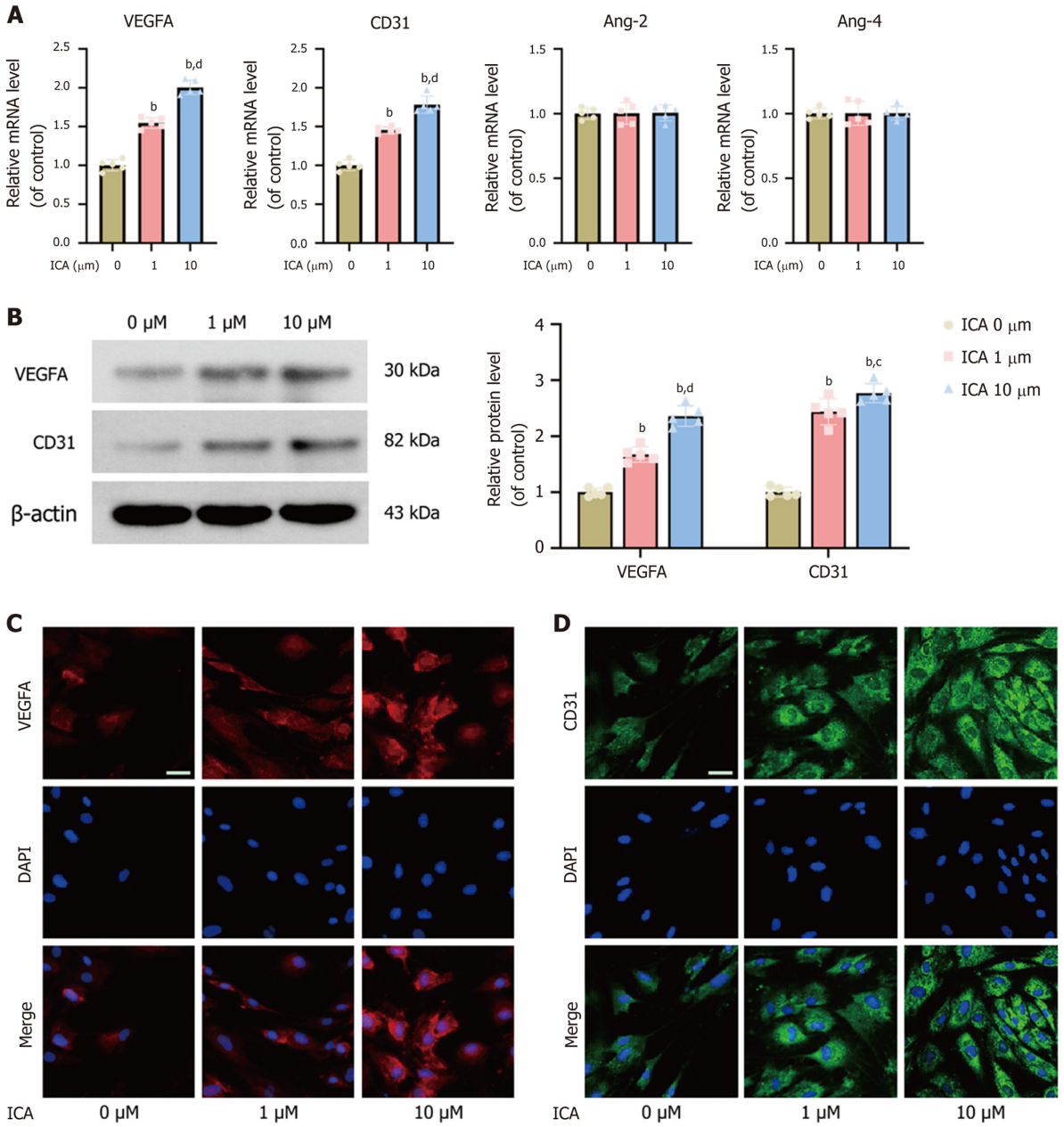

Figure 3 Icariin enhanced the expression of angiogenesis-related markers. A: Expression levels of angiogenesis-related genes [vascular endothelial growth factor A (*VEGFA*), platelet endothelial cell adhesion molecule 1 (*CD31*), angiopoietin-2 *(Ang-2*), and angiopoietin-4 *(Ang-4*)] in bone marrow mesenchymal stem cells (BMSCs) following treatment with icariin (ICA); B: Protein expression levels of VEGFA and CD31 by Western blot; C: Expression of VEGFA by immunofluorescence (scale bar: 100 μm); D: Expression of CD31 by immunofluorescence (scale bar: 100 μm). Data are mean ± SEM (n = 5). $^{b}P < 0.01$ *vs* control group; $^{c}P < 0.05$ and $^{d}P < 0.01$ *vs* 1 μM ICA group. ICA: Icariin; VEGFA: Vascular endothelial growth factor A; CD31: Platelet endothelial cell adhesion molecule 1; Ang-2: Angiopoietin-2; Ang-4: Angiopoietin-4; qRT-PCR: Quantitative real-time polymerase chain reaction.

DISCUSSION

It was widely accepted that the relationship between osteogenesis and angiogenesis is unidirectional[41]. However, later studies indicated that the relationship is actually closely coordinated[42-44]. It is worth noting that DM normally impairs angiogenesis[45-47]. Chinipardaz *et al*[48] observed that angiogenesis was significantly reduced in a fractured region in a T1DM mouse model compared to that in normal mice. The decrease in angiogenesis could suppress trabecular bone regeneration and delay bone healing[49]. Therefore, it is essential to focus on vascular regeneration when studying bone regeneration. Through this study, we discovered that ICA enhanced the expression of osteogenesis-related and angiogenesis-related markers in a T1DM mouse model, and the optimal concentration for promoting osteogenesis and angiogenesis was the same. In addition, although ICA cannot directly promote angiogenesis our results indicated that it can work synergistically with BMSCs to promote angiogenesis.

The connection between BMSCs and endothelial cells is attributed to osteoblastic and angiogenic factor production (*e.g.*, VEGFA)[50], which was consistent with our *in vitro* findings. Our subsequent *in vivo* studies revealed that ICA promoted osteogenesis and H-positive capillary formation in the defect area. Previous studies have observed that H-type

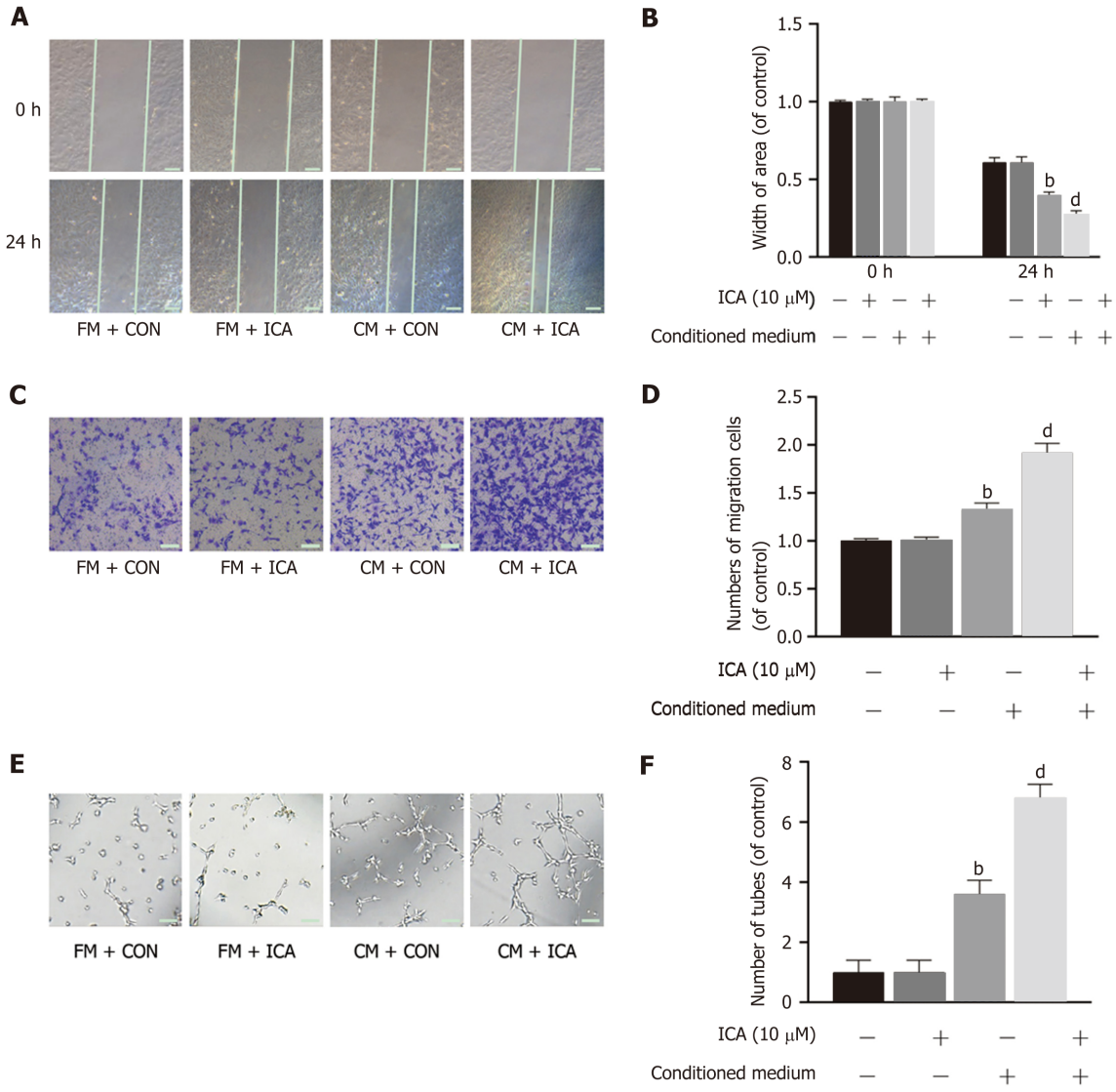

Figure 4 Icariin induced osteogenesis-angiogenesis coupling of bone marrow mesenchymal stem cells. A: Scratch wound assay to show migration of human umbilical vein endothelial cells (HUVECs) cultured with fresh medium (FM) or conditioned medium (CM) and with or without icariin (ICA) (scale bar: 100 μm); B: Quantification of the scratch wound assays; C: Transwell migration assay of HUVECs cultured with FM or CM and with or without ICA (scale bar: 100 μm); D: Quantification of the transwell migration assays; E: Tube formation assay of HUVECs cultured with FM or CM and with or without ICA (scale bar: 100 μm); F: Quantification of the tube formation assays. Data are mean ± SEM (n = 5). $^{b}P < 0.01$ *vs* control group; $^{d}P < 0.01$ *vs* CM + control group. ICA: Icariin; FM: Fresh medium; CM: Conditioned medium; Con: Control.

blood vessels could couple osteogenesis and angiogenesis[51-53]. This indicated that the roles of ICA in promoting osteogenesis and angiogenesis were not independent *in vivo*. They are coupled by H-type blood vessels to play synergistic roles. This study is the first to demonstrate that ICA possesses the ability to induce osteogenesis-angiogenesis coupling in BMSCs.

Natural products with structural diversity and biological activity are important sources of innovative drugs[54]. ICA is a natural flavonol glycoside used in traditional Chinese medicine[55] and research has shown that it can promote osteogenesis in various ways[56-58]. Xia *et al*[59] found that ICA could promote osteogenic differentiation of BMSCs by upregulating GLI-1, and Luo *et al*[60] observed that ICA restored osteogenic differentiation of BMSCs in ovariectomized (commonly known as OVX) rats. A growing body of research has shown that ICA is beneficial in models of diabetes[61-63]. Significantly, the safety of ICA has been demonstrated by multiple studies[64-66]. Thus, ICA is expected to exert more vital roles in improving diabetes and promoting bone regeneration due to its natural origin and safety.

The osteogenic differentiation of BMSCs is important for bone regeneration, and angiogenesis plays an indispensable role during the bone regeneration process[67-69]. Wu *et al*[70] showed that ICA could promote repair of a normal bone defect *via* enhancement of osteogenesis and angiogenesis. In this study, we demonstrated that ICA induced osteogenesis-angiogenesis coupling in BMSCs *in vitro*, and that ICA facilitated bone formation and CD31^{hi}EMCN^{hi} type H-positive capillary formation in the defect area of a T1DM rat model. We used single and double fluorochrome labeling as a direct histologic marker of bone formation. This test showed that in the T1DM model there was a reduced rate of bone formation in the defect area compared to the CON group. When the T1DM rats were treated with ICA, the double fluorochrome labeling demonstrated that ICA accelerated the rate of bone formation in the defect area. Although this study

Table 1 Real-time polymerase chain reaction primer sequences

Gene	Forward primer	Reverse primer
ALP	ACCATTCCCACGTCTTCACATTT	AGACATTCTCTCGTTCACCGCC
OCN	GTCAGACTACAACATCCAGAAG	CGAGTATCTTCCTGTTTGACC
RUNX2	GAGCGTTCAACGGCACAG	GACAGTAGACTCCACGACA
COL1A1	TGTCGTTCAACGGCACAG	TGTGGTAGACTCCACGACA
VEGFA	TCAGGAGGACCTTGTGTGATCAG	CATTGCTCTGTACCTTGGGAA
CD31	CACCGTGATACTGAACAGCAA	GTCACAATCCCACCTTCTGTC
Ang-2	GAAGAAGGAGATGGTGGAGA	CGTCTGGTTGAGCAAACTG
Ang-4	GCTCCTCAGGGCACCAAGTTC	CACAGGCGTCAAACCACCAC
GAPDH	GGCATGGACTGTGGTCATGAG	TGCACCACCAACTGTTAGC

ALP: Alkaline phosphatase; *Ang-2*: Angiopoietin-2; *Ang-4*: Angiopoietin-4; *CD31*: Platelet endothelial cell adhesion molecule 1; *COL1A1*: Collagen type I alpha 1; *GAPDH*: Glyceraldehyde-3-phosphate dehydrogenase; *OCN*: Osteocalcin; *RUNX2*: Runt-related transcription factor 2; *VEGFA*: Vascular endothelial growth factor A.

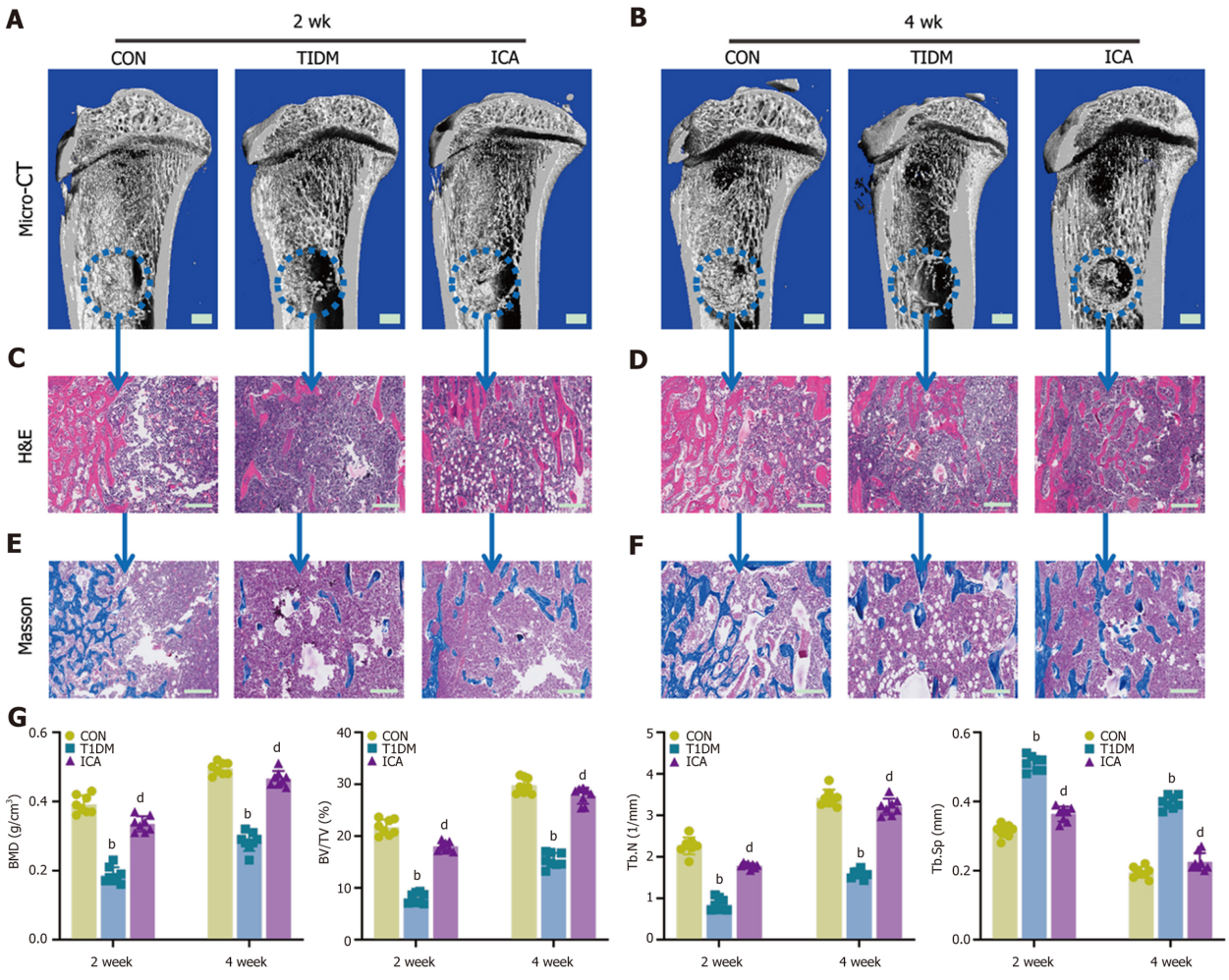

Figure 5 Icariin improved bone repair capacity by promoting osteogenesis in type 1 diabetes mellitus rats. A and B: Three-dimensional reconstruction images of the defect area at week 2 (A) and week 4 (B) (scale bars: 1 mm); C and D: Hematoxylin and eosin staining of the defect area at week 2 (C) and week 4 (B) (scale bars: 200 μm); E and F: Masson's trichrome staining of the defect area at week 2 (E) and week 4 (F) (scale bars: 200 μm); G: Micron-scale computed tomography analysis of bone mineral density (BMD), bone volume/tissue volume (BV/TV), trabecular number (Tb.N), and trabecular separation (Tb.Sp) at weeks 2 and 4. Data are mean ± SEM of the mean (n = 8). $^{b}P < 0.01$ *vs* the control group; $^{d}P < 0.01$ *vs* the type 1 diabetes mellitus group. ICA: Icariin; Con: Control; T1DM: Type 1 diabetes mellitus.

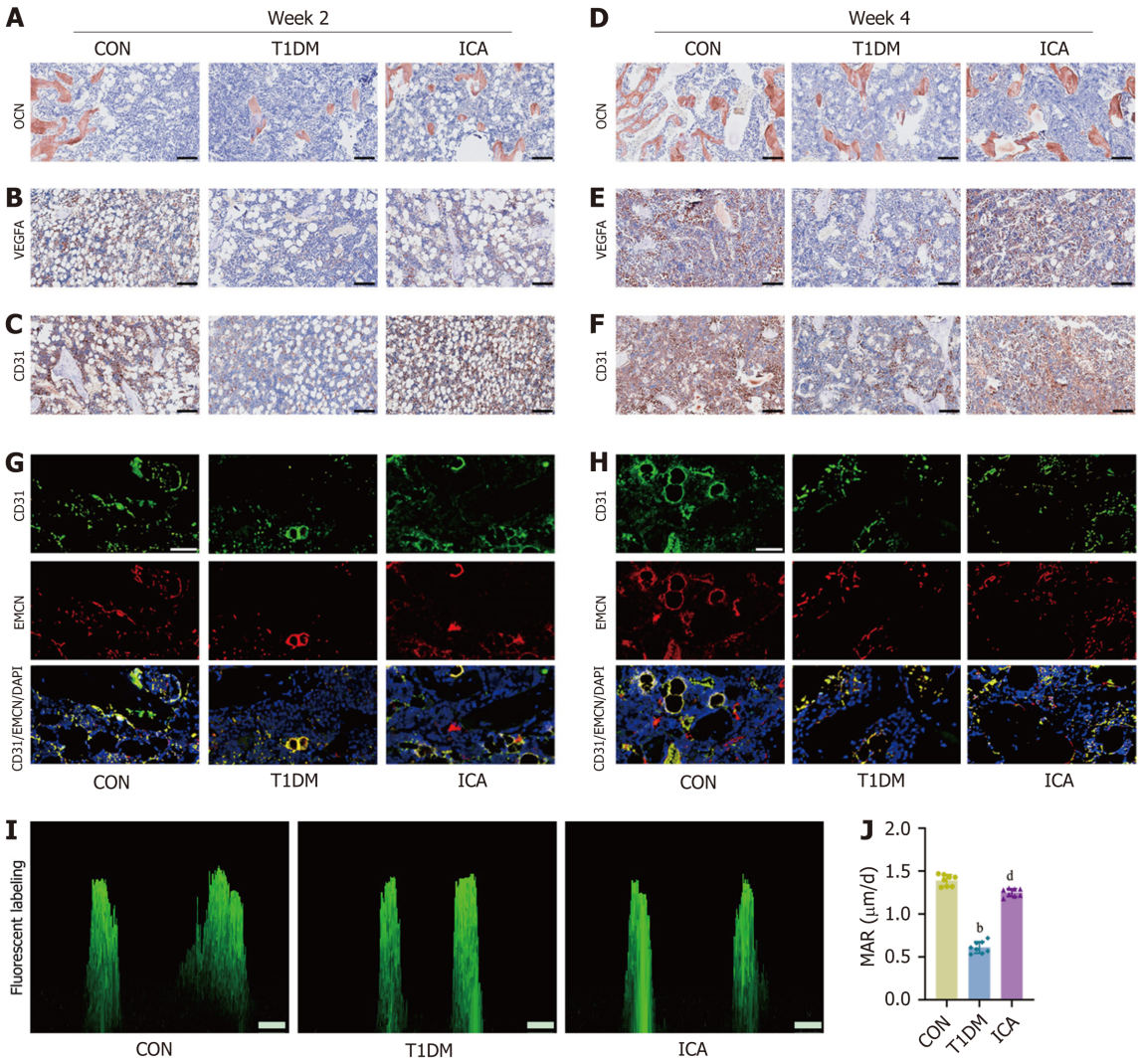

Figure 6 Icariin accelerated bone regeneration by inducing osteogenesis-angiogenesis coupling of bone marrow mesenchymal stem cells in type 1 diabetes mellitus rats. A-C: Immunohistochemical results of osteocalcin (OCN) (A), vascular endothelial growth factor A (VEGFA) (B), and platelet endothelial cell adhesion molecule 1 (CD31) (C) in the defect area at week 2 (scale bars: 100 μm); D-F: Immunohistochemical results of OCN (D), VEGFA (E), and CD31 (F) in the defect area at week 4 (scale bars: 100 μm); G: CD31 and endomucin (EMCN) double immunofluorescence staining in the defect area at week 2 (scale bar: 100 μm); H: CD31 and EMCN double immunofluorescence staining in the defect area at week 4 (scale bar: 100 μm); I: Sequential fluorescent labeling (scale bar: 10 μm); J: Quantitative analysis of mineral apposition rate. Data are mean ± SEM (n = 8). $^{b}P < 0.01$ *vs* the control group; $^{d}P < 0.01$ *vs* the type 1 diabetes mellitus group. ICA: Icariin; Con: Control; T1DM: Type 1 diabetes mellitus; OCN: Osteocalcin; VEGFA: Vascular endothelial growth factor A; CD31: Platelet endothelial cell adhesion molecule 1.

revealed that the pro-osteogenesis effect of ICA is strictly connected to its pro-angiogenesis effect and together contribute to the bone regeneration in the context of TIDM, the effects of ICA on bone resorption and bone homeostasis were not investigated; indeed, these latter topics are the focus of our ongoing research.

CONCLUSION

Taken together, we conclude that ICA could accelerate bone regeneration by inducing osteogenesis-angiogenesis coupling of BMSCs in the T1DM rat model. This finding also implies that ICA may be a potential drug for treating bone defect in the context of TIDM, and more importantly that further investigations into the effective coupling of osteogenesis and angiogenesis should be undertaken in the field of bone regeneration in T1DM patients.

ARTICLE HIGHLIGHTS

Research background

Icariin (ICA) has multiple pharmacological activities. However, its effect on bone defect repair in the context of type 1 diabetes mellitus (T1DM) remains unclear.

Research motivation

ICA possesses the ability to promote osteogenesis and exert protective effects in T1DM. Therefore, ICA may have therapeutic potential for repairing bone defects in patients with T1DM.

Research objectives

To explore the role of ICA on bone defect repair in T1DM models.

Research methods

The effects of ICA on osteogenesis and angiogenesis were evaluated by molecular biology techniques *in vitro*. After a T1DM rat model was established, we evaluated the effect of ICA on bone formation in a defect area.

Research results

ICA promoted bone marrow mesenchymal stem cell (BMSC) osteogenic differentiation and induced osteogenesis-angiogenesis coupling of BMSCs *in vitro*. Subsequently, we observed that ICA facilitated bone formation and type H vessel formation in the defect area of the T1DM rat model. Sequential fluorescent labeling confirmed that ICA could effectively accelerate the rate of bone formation in the defect area.

Research conclusions

ICA accelerated bone regeneration by inducing osteogenesis-angiogenesis coupling of BMSCs in the T1DM rat model.

Research perspectives

Our study highlighted the importance of effective coupling of osteogenesis and angiogenesis in bone regeneration in the context of T1DM.

FOOTNOTES

Co-corresponding authors: Jia Zheng and Yi-Kai Li.

Author contributions: Zheng J and Li YK contributed equally to this work and are co-corresponding authors on this paper according to the critical roles they played throughout the research in experimental design, data analysis, and provision of intellectual ideas and methods; Zheng S, Zheng J, and Li YK designed the research study; Zheng S, Hu GY, and Li JH performed the research; Li JH and Zheng J contributed new reagents and analytic tools; Zheng S, Zheng J, and Li YK analyzed the data and wrote the manuscript; and all authors read and approved the final manuscript.

Supported by the Postdoctoral Fellowship Program of China Postdoctoral Science Foundation, No. GZC20231088; and President Foundation of The Third Affiliated Hospital of Southern Medical University, China, No. YP202210.

Institutional animal care and use committee statement: The study was reviewed and approved by the Animal Ethics Committee of Southern Medical University (Approval No. SMUL2022023).

Conflict-of-interest statement: The authors declare having no competing interests for this article.

Data sharing statement: Data will be made available upon reasonable request to the corresponding author.

ARRIVE guidelines statement: The authors have read the ARRIVE guidelines, and the manuscript was prepared and revised according to the ARRIVE guidelines.

Country/Territory of origin: China

ORCID number: Sheng Zheng 0000-0001-6525-8721; Guan-Yu Hu 0000-0002-1148-0631; Jun-Hua Li 0000-0001-6860-3877; Jia Zheng 0000-0002-6480-3422; Yi-Kai Li 0000-0003-0766-6051.

S-Editor: Chen YL

L-Editor: A
P-Editor: Zhang YL

REFERENCES

1 **Cuadros DF**, Li J, Musuka G, Awad SF. Spatial epidemiology of diabetes: Methods and insights. *World J Diabetes* 2021; **12**: 1042-1056 [PMID: 34326953 DOI: 10.4239/wjd.v12.i7.1042]
2 **Saeedi P**, Petersohn I, Salpea P, Malanda B, Karuranga S, Unwin N, Colagiuri S, Guariguata L, Motala AA, Ogurtsova K, Shaw JE, Bright D, Williams R; IDF Diabetes Atlas Committee. Global and regional diabetes prevalence estimates for 2019 and projections for 2030 and 2045: Results from the International Diabetes Federation Diabetes Atlas, 9(th) edition. *Diabetes Res Clin Pract* 2019; **157**: 107843 [PMID: 31518657 DOI: 10.1016/j.diabres.2019.107843]
3 **He Y**, Al-Mureish A, Wu N. Nanotechnology in the Treatment of Diabetic Complications: A Comprehensive Narrative Review. *J Diabetes Res* 2021; **2021**: 6612063 [PMID: 34007847 DOI: 10.1155/2021/6612063]
4 **Ben-Assuli O**. Measuring the cost-effectiveness of using telehealth for diabetes management: A narrative review of methods and findings. *Int J Med Inform* 2022; **163**: 104764 [PMID: 35439671 DOI: 10.1016/j.ijmedinf.2022.104764]
5 **Haralambiev L**, Nitsch A, Fischer CS, Lange A, Klöting I, Stope MB, Ekkernkamp A, Lange J. Increase in Bone Mass Before Onset of Type 1 Diabetes Mellitus in Rats. *In Vivo* 2022; **36**: 1077-1082 [PMID: 35478116 DOI: 10.21873/invivo.12805]
6 **Brunetti G**, D'Amato G, De Santis S, Grano M, Faienza MF. Mechanisms of altered bone remodeling in children with type 1 diabetes. *World J Diabetes* 2021; **12**: 997-1009 [PMID: 34326950 DOI: 10.4239/wjd.v12.i7.997]
7 **Wang H**, Akbari-Alavijeh S, Parhar RS, Gaugler R, Hashmi S. Partners in diabetes epidemic: A global perspective. *World J Diabetes* 2023; **14**: 1463-1477 [PMID: 37970124 DOI: 10.4239/wjd.v14.i10.1463]
8 **Kumar S**, Wan C, Ramaswamy G, Clemens TL, Ponnazhagan S. Mesenchymal stem cells expressing osteogenic and angiogenic factors synergistically enhance bone formation in a mouse model of segmental bone defect. *Mol Ther* 2010; **18**: 1026-1034 [PMID: 20068549 DOI: 10.1038/mt.2009.315]
9 **Eldisoky RH**, Younes SA, Omar SS, Gharib HS, Tamara TA. Hyperbaric oxygen therapy efficacy on mandibular defect regeneration in rats with diabetes mellitus: an animal study. *BMC Oral Health* 2023; **23**: 101 [PMID: 36793042 DOI: 10.1186/s12903-023-02801-w]
10 **Dias PC**, Limirio PHJO, Linhares CRB, Bergamini ML, Rocha FS, Morais RB, Balbi APC, Hiraki KRN, Dechichi P. Hyperbaric Oxygen therapy effects on bone regeneration in Type 1 diabetes mellitus in rats. *Connect Tissue Res* 2018; **59**: 574-580 [PMID: 29378458 DOI: 10.1080/03008207.2018.1434166]
11 **Camacho-Alonso F**, Martínez-Ortiz C, Plazas-Buendía L, Mercado-Díaz AM, Vilaplana-Vivo C, Navarro JA, Buendía AJ, Merino JJ, Martínez-Beneyto Y. Bone union formation in the rat mandibular symphysis using hydroxyapatite with or without simvastatin: effects on healthy, diabetic, and osteoporotic rats. *Clin Oral Investig* 2020; **24**: 1479-1491 [PMID: 31925587 DOI: 10.1007/s00784-019-03180-9]
12 **Camacho-Alonso F**, Tudela-Mulero MR, Buendía AJ, Navarro JA, Pérez-Sayáns M, Mercado-Díaz AM. Bone regeneration in critical-sized mandibular symphysis defects using bioceramics with or without bone marrow mesenchymal stem cells in healthy, diabetic, osteoporotic, and diabetic-osteoporotic rats. *Dent Mater* 2022; **38**: 1283-1300 [PMID: 35717229 DOI: 10.1016/j.dental.2022.06.019]
13 **Wang W**, Yeung KWK. Bone grafts and biomaterials substitutes for bone defect repair: A review. *Bioact Mater* 2017; **2**: 224-247 [PMID: 29744432 DOI: 10.1016/j.bioactmat.2017.05.007]
14 **Weffort D**, Adolpho LF, Souza ATP, Freitas GP, Lopes HB, Oliveira FS, Bighetti-Trevisan RL, Pitol-Palin L, Matsushita DH, Okamoto R, Beloti MM, Rosa AL. Normoglycemia partially recovers the disrupted osteoblast differentiation of mesenchymal stem cells induced by type 1 but not type 2 diabetes mellitus. *J Cell Biochem* 2023; **124**: 1050-1063 [PMID: 37293736 DOI: 10.1002/jcb.30434]
15 **Palui R**, Pramanik S, Mondal S, Ray S. Critical review of bone health, fracture risk and management of bone fragility in diabetes mellitus. *World J Diabetes* 2021; **12**: 706-729 [PMID: 34168723 DOI: 10.4239/wjd.v12.i6.706]
16 **Dixit M**, Liu Z, Poudel SB, Yildirim G, Zhang YZ, Mehta S, Murik O, Altarescu G, Kobayashi Y, Shimizu E, Schaffler MB, Yakar S. Skeletal Response to Insulin in the Naturally Occurring Type 1 Diabetes Mellitus Mouse Model. *JBMR Plus* 2021; **5**: e10483 [PMID: 33977201 DOI: 10.1002/jbm4.10483]
17 **Xu S**, Zhao S, Jian Y, Shao X, Han D, Zhang F, Liang C, Liu W, Fan J, Yang Z, Zhou J, Zhang W, Wang Y. Icariin-loaded hydrogel with concurrent chondrogenesis and anti-inflammatory properties for promoting cartilage regeneration in a large animal model. *Front Cell Dev Biol* 2022; **10**: 1011260 [PMID: 36506090 DOI: 10.3389/fcell.2022.1011260]
18 **Bi Z**, Zhang W, Yan X. Anti-inflammatory and immunoregulatory effects of icariin and icaritin. *Biomed Pharmacother* 2022; **151**: 113180 [PMID: 35676785 DOI: 10.1016/j.biopha.2022.113180]
19 **Su BL**, Wang LL, Zhang LY, Zhang S, Li Q, Chen GY. Potential role of microRNA-503 in Icariin-mediated prevention of high glucose-induced endoplasmic reticulum stress. *World J Diabetes* 2023; **14**: 1234-1248 [PMID: 37664468 DOI: 10.4239/wjd.v14.i8.1234]
20 **Jin J**, Wang H, Hua X, Chen D, Huang C, Chen Z. An outline for the pharmacological effect of icariin in the nervous system. *Eur J Pharmacol* 2019; **842**: 20-32 [PMID: 30342950 DOI: 10.1016/j.ejphar.2018.10.006]
21 **Verma A**, Aggarwal K, Agrawal R, Pradhan K, Goyal A. Molecular mechanisms regulating the pharmacological actions of icariin with special focus on PI3K-AKT and Nrf-2 signaling pathways. *Mol Biol Rep* 2022; **49**: 9023-9032 [PMID: 35941411 DOI: 10.1007/s11033-022-07778-3]
22 **Xu H**, Zhou S, Qu R, Yang Y, Gong X, Hong Y, Jin A, Huang X, Dai Q, Jiang L. Icariin prevents oestrogen deficiency-induced alveolar bone loss through promoting osteogenesis *via* STAT3. *Cell Prolif* 2020; **53**: e12743 [PMID: 31943455 DOI: 10.1111/cpr.12743]
23 **Xu Y**, Jiang Y, Jia B, Wang Y, Li T. Icariin stimulates osteogenesis and suppresses adipogenesis of human bone mesenchymal stem cells *via* miR-23a-mediated activation of the Wnt/β-catenin signaling pathway. *Phytomedicine* 2021; **85**: 153485 [PMID: 33743412 DOI: 10.1016/j.phymed.2021.153485]
24 **He C**, Wang Z, Shi J. Pharmacological effects of icariin. *Adv Pharmacol* 2020; **87**: 179-203 [PMID: 32089233 DOI: 10.1016/bs.apha.2019.10.004]
25 **Huang Z**, Wei H, Wang X, Xiao J, Li Z, Xie Y, Hu Y, Li X, Wang Z, Zhang S. Icariin promotes osteogenic differentiation of BMSCs by upregulating BMAL1 expression *via* BMP signaling. *Mol Med Rep* 2020; **21**: 1590-1596 [PMID: 32016461 DOI: 10.3892/mmr.2020.10954]
26 **Cheng L**, Jin X, Shen H, Chen X, Chen J, Xu B, Xu J. Icariin attenuates thioacetamideinduced bone loss *via* the RANKLp38/ERKNFAT

signaling pathway. *Mol Med Rep* 2022; **25** [PMID: 35169865 DOI: 10.3892/mmr.2022.12642]
27 **Hao FL**, Mei S, Liu X, Liu Y, Zhang XD, Dong FS. Icariin contributes to healing skull defects in rabbit model. *J Tradit Chin Med* 2021; **41**: 471-478 [PMID: 34114406 DOI: 10.19852/j.cnki.jtcm.2021.03.016]
28 **Du W**, Tang Z, Yang F, Liu X, Dong J. Icariin attenuates bleomycin-induced pulmonary fibrosis by targeting Hippo/YAP pathway. *Biomed Pharmacother* 2021; **143**: 112152 [PMID: 34536758 DOI: 10.1016/j.biopha.2021.112152]
29 **Yao W**, Wang K, Wang X, Li X, Dong J, Zhang Y, Ding X. Icariin ameliorates endothelial dysfunction in type 1 diabetic rats by suppressing ER stress *via* the PPARα/Sirt1/AMPKα pathway. *J Cell Physiol* 2021; **236**: 1889-1902 [PMID: 32770555 DOI: 10.1002/jcp.29972]
30 **Lu CS**, Wu CY, Wang YH, Hu QQ, Sun RY, Pan MJ, Lu XY, Zhu T, Luo S, Yang HJ, Wang D, Wang HW. The protective effects of icariin against testicular dysfunction in type 1 diabetic mice Via AMPK-mediated Nrf2 activation and NF-κB p65 inhibition. *Phytomedicine* 2024; **123**: 155217 [PMID: 37992492 DOI: 10.1016/j.phymed.2023.155217]
31 **Grellier M**, Granja PL, Fricain JC, Bidarra SJ, Renard M, Bareille R, Bourget C, Amédée J, Barbosa MA. The effect of the co-immobilization of human osteoprogenitors and endothelial cells within alginate microspheres on mineralization in a bone defect. *Biomaterials* 2009; **30**: 3271-3278 [PMID: 19299013 DOI: 10.1016/j.biomaterials.2009.02.033]
32 **Zhang D**, Zhao N, Wan C, Du J, Lin J, Wang H. Icariin and Icariside II Reciprocally Stimulate Osteogenesis and Inhibit Adipogenesis of Multipotential Stromal Cells through ERK Signaling. *Evid Based Complement Alternat Med* 2021; **2021**: 8069930 [PMID: 34956384 DOI: 10.1155/2021/8069930]
33 **Zhang JT**, Zhang SS, Liu CG, Kankala RK, Chen AZ, Wang SB. Low-temperature extrusion-based 3D printing of icariin-laden scaffolds for osteogenesis enrichment. *Regen Ther* 2021; **16**: 53-62 [PMID: 33521173 DOI: 10.1016/j.reth.2021.01.001]
34 **Xie L**, Liu N, Xiao Y, Liu Y, Yan C, Wang G, Jing X. In Vitro and In Vivo Osteogenesis Induced by Icariin and Bone Morphogenetic Protein-2: A Dynamic Observation. *Front Pharmacol* 2020; **11**: 1058 [PMID: 32760277 DOI: 10.3389/fphar.2020.01058]
35 **Yu H**, Yue J, Wang W, Liu P, Zuo W, Guo W, Zhang Q. Icariin promotes angiogenesis in glucocorticoid-induced osteonecrosis of femoral heads: In vitro and *in vivo* studies. *J Cell Mol Med* 2019; **23**: 7320-7330 [PMID: 31507078 DOI: 10.1111/jcmm.14589]
36 **Huang H**, Zhang ZF, Qin FW, Tang W, Liu DH, Wu PY, Jiao F. Icariin inhibits chondrocyte apoptosis and angiogenesis by regulating the TDP-43 signaling pathway. *Mol Genet Genomic Med* 2019; **7**: e00586 [PMID: 30734541 DOI: 10.1002/mgg3.586]
37 **Zheng S**, Zhou C, Yang H, Li J, Feng Z, Liao L, Li Y. Melatonin Accelerates Osteoporotic Bone Defect Repair by Promoting Osteogenesis-Angiogenesis Coupling. *Front Endocrinol (Lausanne)* 2022; **13**: 826660 [PMID: 35273570 DOI: 10.3389/fendo.2022.826660]
38 **Furman BL**. Streptozotocin-Induced Diabetic Models in Mice and Rats. *Curr Protoc* 2021; **1**: e78 [PMID: 33905609 DOI: 10.1002/cpz1.78]
39 **Qi S**, He J, Zheng H, Chen C, Lan S. Icariin Prevents Diabetes-Induced Bone Loss in Rats by Reducing Blood Glucose and Suppressing Bone Turnover. *Molecules* 2019; **24** [PMID: 31096652 DOI: 10.3390/molecules24101871]
40 **Tao ZS**, Lu HL, Ma NF, Zhang RT, Li Y, Yang M, Xu HG. Rapamycin could increase the effects of melatonin against age-dependent bone loss. *Z Gerontol Geriatr* 2020; **53**: 671-678 [PMID: 31781847 DOI: 10.1007/s00391-019-01659-4]
41 **Lafage-Proust MH**, Prisby R, Roche B, Vico L. Bone vascularization and remodeling. *Joint Bone Spine* 2010; **77**: 521-524 [PMID: 20980183 DOI: 10.1016/j.jbspin.2010.09.009]
42 **Dhandapani R**, Krishnan PD, Zennifer A, Kannan V, Manigandan A, Arul MR, Jaiswal D, Subramanian A, Kumbar SG, Sethuraman S. Additive manufacturing of biodegradable porous orthopaedic screw. *Bioact Mater* 2020; **5**: 458-467 [PMID: 32280835 DOI: 10.1016/j.bioactmat.2020.03.009]
43 **Kusumbe AP**, Ramasamy SK, Adams RH. Coupling of angiogenesis and osteogenesis by a specific vessel subtype in bone. *Nature* 2014; **507**: 323-328 [PMID: 24646994 DOI: 10.1038/nature13145]
44 **Zhao Y**, Xie L. Unique bone marrow blood vessels couple angiogenesis and osteogenesis in bone homeostasis and diseases. *Ann N Y Acad Sci* 2020; **1474**: 5-14 [PMID: 32242943 DOI: 10.1111/nyas.14348]
45 **Yan C**, Chen J, Wang C, Yuan M, Kang Y, Wu Z, Li W, Zhang G, Machens HG, Rinkevich Y, Chen Z, Yang X, Xu X. Milk exosomes-mediated miR-31-5p delivery accelerates diabetic wound healing through promoting angiogenesis. *Drug Deliv* 2022; **29**: 214-228 [PMID: 34985397 DOI: 10.1080/10717544.2021.2023699]
46 **Wang Y**, Cao Z, Wei Q, Ma K, Hu W, Huang Q, Su J, Li H, Zhang C, Fu X. VH298-loaded extracellular vesicles released from gelatin methacryloyl hydrogel facilitate diabetic wound healing by HIF-1α-mediated enhancement of angiogenesis. *Acta Biomater* 2022; **147**: 342-355 [PMID: 35580827 DOI: 10.1016/j.actbio.2022.05.018]
47 **Tang X**, Luo Y, Yuan D, Calandrelli R, Malhi NK, Sriram K, Miao Y, Lou CH, Tsark W, Tapia A, Chen AT, Zhang G, Roeth D, Kalkum M, Wang ZV, Chien S, Natarajan R, Cooke JP, Zhong S, Chen ZB. Long noncoding RNA LEENE promotes angiogenesis and ischemic recovery in diabetes models. *J Clin Invest* 2023; **133** [PMID: 36512424 DOI: 10.1172/JCI161759]
48 **Chinipardaz Z**, Liu M, Graves D, Yang S. Diabetes impairs fracture healing through disruption of cilia formation in osteoblasts. *Bone* 2021; **153**: 116176 [PMID: 34508881 DOI: 10.1016/j.bone.2021.116176]
49 **Huang B**, Wang W, Li Q, Wang Z, Yan B, Zhang Z, Wang L, Huang M, Jia C, Lu J, Liu S, Chen H, Li M, Cai D, Jiang Y, Jin D, Bai X. Osteoblasts secrete Cxcl9 to regulate angiogenesis in bone. *Nat Commun* 2016; **7**: 13885 [PMID: 27966526 DOI: 10.1038/ncomms13885]
50 **Leach JK**, Kaigler D, Wang Z, Krebsbach PH, Mooney DJ. Coating of VEGF-releasing scaffolds with bioactive glass for angiogenesis and bone regeneration. *Biomaterials* 2006; **27**: 3249-3255 [PMID: 16490250 DOI: 10.1016/j.biomaterials.2006.01.033]
51 **Ramasamy SK**, Kusumbe AP, Wang L, Adams RH. Endothelial Notch activity promotes angiogenesis and osteogenesis in bone. *Nature* 2014; **507**: 376-380 [PMID: 24647000 DOI: 10.1038/nature13146]
52 **Xu R**, Yallowitz A, Qin A, Wu Z, Shin DY, Kim JM, Debnath S, Ji G, Bostrom MP, Yang X, Zhang C, Dong H, Kermani P, Lalani S, Li N, Liu Y, Poulos MG, Wach A, Zhang Y, Inoue K, Di Lorenzo A, Zhao B, Butler JM, Shim JH, Glimcher LH, Greenblatt MB. Targeting skeletal endothelium to ameliorate bone loss. *Nat Med* 2018; **24**: 823-833 [PMID: 29785024 DOI: 10.1038/s41591-018-0020-z]
53 **Yang M**, Li CJ, Sun X, Guo Q, Xiao Y, Su T, Tu ML, Peng H, Lu Q, Liu Q, He HB, Jiang TJ, Lei MX, Wan M, Cao X, Luo XH. MiR-497~195 cluster regulates angiogenesis during coupling with osteogenesis by maintaining endothelial Notch and HIF-1α activity. *Nat Commun* 2017; **8**: 16003 [PMID: 28685750 DOI: 10.1038/ncomms16003]
54 **Li Y**, Zhang L, Wang W, Liu Y, Sun D, Li H, Chen L. A review on natural products with cage-like structure. *Bioorg Chem* 2022; **128**: 106106 [PMID: 36037599 DOI: 10.1016/j.bioorg.2022.106106]
55 **Wang S**, Ma J, Zeng Y, Zhou G, Wang Y, Zhou W, Sun X, Wu M. Icariin, an Up-and-Coming Bioactive Compound Against Neurological Diseases: Network Pharmacology-Based Study and Literature Review. *Drug Des Devel Ther* 2021; **15**: 3619-3641 [PMID: 34447243 DOI: 10.2147/DDDT.S310686]

56 **Chai H**, Sang S, Luo Y, He R, Yuan X, Zhang X. Icariin-loaded sulfonated polyetheretherketone with osteogenesis promotion and osteoclastogenesis inhibition properties *via* immunomodulation for advanced osseointegration. *J Mater Chem B* 2022; **10**: 3531-3540 [PMID: 35416810 DOI: 10.1039/d1tb02802b]

57 **Gao J**, Xiang S, Wei X, Yadav RI, Han M, Zheng W, Zhao L, Shi Y, Cao Y. Icariin Promotes the Osteogenesis of Bone Marrow Mesenchymal Stem Cells through Regulating Sclerostin and Activating the Wnt/β-Catenin Signaling Pathway. *Biomed Res Int* 2021; **2021**: 6666836 [PMID: 33553429 DOI: 10.1155/2021/6666836]

58 **Wu Y**, Xia L, Zhou Y, Ma W, Zhang N, Chang J, Lin K, Xu Y, Jiang X. Evaluation of osteogenesis and angiogenesis of icariin loaded on micro/nano hybrid structured hydroxyapatite granules as a local drug delivery system for femoral defect repair. *J Mater Chem B* 2015; **3**: 4871-4883 [PMID: 32262676 DOI: 10.1039/c5tb00621j]

59 **Xia SL**, Ma ZY, Wang B, Gao F, Guo SY, Chen XH. Icariin promotes the proliferation and osteogenic differentiation of bone-derived mesenchymal stem cells in patients with osteoporosis and T2DM by upregulating GLI-1. *J Orthop Surg Res* 2023; **18**: 500 [PMID: 37454090 DOI: 10.1186/s13018-023-03998-w]

60 **Luo Z**, Liu M, Sun L, Rui F. Icariin recovers the osteogenic differentiation and bone formation of bone marrow stromal cells from a rat model of estrogen deficiency-induced osteoporosis. *Mol Med Rep* 2015; **12**: 382-388 [PMID: 25695835 DOI: 10.3892/mmr.2015.3369]

61 **Jiang W**, Ding K, Yue R, Lei M. Therapeutic effects of icariin and icariside II on diabetes mellitus and its complications. *Crit Rev Food Sci Nutr* 2023; 1-26 [PMID: 36591787 DOI: 10.1080/10408398.2022.2159317]

62 **Liu J**, Cheng Q, Wu X, Zhu H, Deng X, Wang M, Yang S, Xu J, Chen Q, Li M, Liu X, Wang C. Icariin Treatment Rescues Diabetes Induced Bone Loss *via* Scavenging ROS and Activating Primary Cilia/Gli2/Osteocalcin Signaling Pathway. *Cells* 2022; **11** [PMID: 36552853 DOI: 10.3390/cells11244091]

63 **Ni T**, Lin N, Huang X, Lu W, Sun Z, Zhang J, Lin H, Chi J, Guo H. Icariin Ameliorates Diabetic Cardiomyopathy Through Apelin/Sirt3 Signalling to Improve Mitochondrial Dysfunction. *Front Pharmacol* 2020; **11**: 256 [PMID: 32265695 DOI: 10.3389/fphar.2020.00256]

64 **Desai TD**, Wen YT, Daddam JR, Cheng F, Chen CC, Pan CL, Lin KL, Tsai RK. Long term therapeutic effects of icariin-loaded PLGA microspheres in an experimental model of optic nerve ischemia *via* modulation of CEBP-β/G-CSF/noncanonical NF-κB axis. *Bioeng Transl Med* 2022; **7**: e10289 [PMID: 35600664 DOI: 10.1002/btm2.10289]

65 **Liu L**, Zhao C, Zhao S, Xu H, Peng Z, Zhang B, Cai W, Mo Y, Zhao W. Evaluation of the effectiveness and safety of icariin in the treatment of knee osteoarthritis: A protocol for a systematic review and meta-analysis. *Medicine (Baltimore)* 2021; **100**: e28277 [PMID: 34918702 DOI: 10.1097/MD.0000000000028277]

66 **Liu FY**, Ding DN, Wang YR, Liu SX, Peng C, Shen F, Zhu XY, Li C, Tang LP, Han FJ. Icariin as a potential anticancer agent: a review of its biological effects on various cancers. *Front Pharmacol* 2023; **14**: 1216363 [PMID: 37456751 DOI: 10.3389/fphar.2023.1216363]

67 **Chen L**, Zhang RY, Xie J, Yang JY, Fang KH, Hong CX, Yang RB, Bsoul N, Yang L. STAT3 activation by catalpol promotes osteogenesis-angiogenesis coupling, thus accelerating osteoporotic bone repair. *Stem Cell Res Ther* 2021; **12**: 108 [PMID: 33541442 DOI: 10.1186/s13287-021-02178-z]

68 **Mousaei Ghasroldasht M**, Matin MM, Kazemi Mehrjerdi H, Naderi-Meshkin H, Moradi A, Rajabioun M, Alipour F, Ghasemi S, Zare M, Mirahmadi M, Bidkhori HR, Bahrami AR. Application of mesenchymal stem cells to enhance non-union bone fracture healing. *J Biomed Mater Res A* 2019; **107**: 301-311 [PMID: 29673055 DOI: 10.1002/jbm.a.36441]

69 **Wang F**, Qian H, Kong L, Wang W, Wang X, Xu Z, Chai Y, Xu J, Kang Q. Accelerated Bone Regeneration by Astragaloside IV through Stimulating the Coupling of Osteogenesis and Angiogenesis. *Int J Biol Sci* 2021; **17**: 1821-1836 [PMID: 33994865 DOI: 10.7150/ijbs.57681]

70 **Wu Y**, Cao L, Xia L, Wu Q, Wang J, Wang X, Xu L, Zhou Y, Xu Y, Jiang X. Evaluation of Osteogenesis and Angiogenesis of Icariin in Local Controlled Release and Systemic Delivery for Calvarial Defect in Ovariectomized Rats. *Sci Rep* 2017; **7**: 5077 [PMID: 28698566 DOI: 10.1038/s41598-017-05392-z]

Published by **Baishideng Publishing Group Inc**
7041 Koll Center Parkway, Suite 160, Pleasanton, CA 94566, USA
Telephone: +1-925-3991568
E-mail: office@baishideng.com
Help Desk: https://www.f6publishing.com/helpdesk
https://www.wjgnet.com